

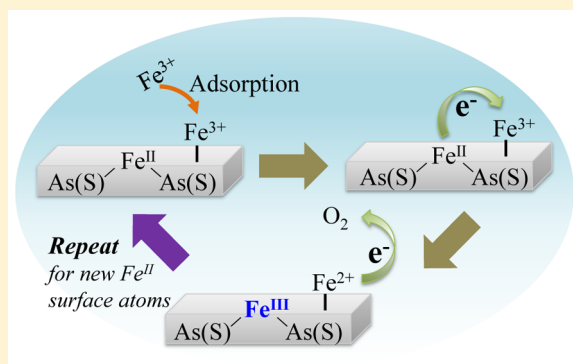
# Fe<sup>3+</sup> Addition Promotes Arsenopyrite Dissolution and Iron(III) (hydr)oxide Formation and Phase Transformation

Chelsea W. Neil and Young-Shin Jun\*

Department of Energy, Environmental & Chemical Engineering, Washington University in St. Louis, One Brookings Drive, Campus Box 1180, St. Louis, Missouri 63130, United States

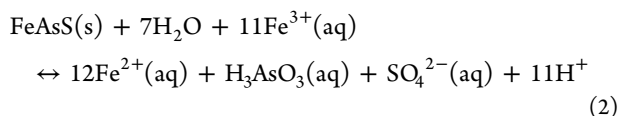
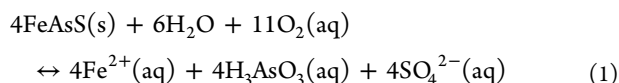
**S** Supporting Information

**ABSTRACT:** The oxidative dissolution of arsenic-containing pyrite is an important process controlling arsenic fate and transport in groundwater aquifers. This process is further complicated by iron(III) (hydr)oxide formation during pyrite oxidation, which can serve as a crucial sink for mobilized arsenic. This study examines the oxidative dissolution of arsenopyrite in the presence of Fe<sup>3+</sup> at circumneutral pH. We show for the first time that despite their low solubility, small quantities of additional Fe<sup>3+</sup> trigger electron transfer between Fe<sup>3+</sup> and Fe(II) in arsenopyrite, resulting in higher extents of secondary mineral formation and faster phase transformation. In addition, dissolved arsenic concentrations are elevated in these systems because of faster dissolution and faster phase transformation. These findings have significant environmental implications for arsenic transport under dynamic redox conditions, where interactions between Fe<sup>3+</sup> and arsenopyrite can dominate arsenic-bearing pyrite oxidation as well as iron(III) (hydr)oxide formation and stability.



## INTRODUCTION

The oxidative dissolution of arsenic-containing pyrite crucially affects the fate and transport of arsenic in groundwater and surface water systems. According to the World Health Organization, more than 137 million people worldwide are affected by arsenic contamination of drinking water, leading to increased risks of cancer.<sup>1</sup> Elevated arsenic levels frequently result from biogeochemical processes mobilizing arsenic from naturally occurring minerals in the sediment.<sup>2–4</sup> These minerals include iron sulfides, such as arsenopyrite (FeAsS) and arsenian pyrite [Fe(As,S)<sub>2</sub>, where the As content is <1–10%].<sup>5</sup> Arsenopyrite can be oxidized by dissolved oxygen and by Fe<sup>3+</sup>(aq) through the following mechanisms:<sup>6,7</sup>



The oxidation of arsenic-containing pyrite is extremely complex because of the simultaneous mobilization of arsenic and iron.<sup>8–10</sup> Under oxidizing conditions, aqueous Fe<sup>2+</sup> (eqs 1 and 2) oxidizes to form Fe<sup>3+</sup>, which can be further hydrolyzed in aquatic systems to form iron(III) (hydr)oxide secondary mineral precipitates.<sup>7</sup> These precipitates can attenuate arsenic through adsorption and coprecipitation, acting as natural sinks. In this letter, we express the oxidation state of solid phases as

Roman numerals and the oxidation state of aqueous and sorbed species as Arabic numerals. In addition, the term “dissolved (or aqueous) Fe<sup>3+</sup> species” is used to describe any reactive hydroxo–Fe<sup>3+</sup> aqueous complexes, such as Fe(OH)<sub>2</sub><sup>+</sup> or Fe(OH)<sub>3</sub>(aq), rather than just free Fe<sup>3+</sup>(aq) cations. The term “Fe<sup>3+</sup>” is used to describe both colloidal Fe(III) phases and hydroxo–Fe<sup>3+</sup> aqueous complexes.

Many previous studies have shown that Fe<sup>2+</sup> can catalyze the phase transformation of iron(III) (hydr)oxides,<sup>11–15</sup> and Fe<sup>2+</sup> from arsenopyrite dissolution can potentially act in the same manner. For instance, Burton et al.<sup>15</sup> studied the effect of Fe<sup>2+</sup>-catalyzed phase transformation on arsenic associated with the Fe(III) mineral precursors and found that the arsenate became more tightly bound in the crystallized product phases after phase transformation. While these studies have considered the effects of aqueous Fe<sup>2+</sup> on iron(III) (hydr)oxides, more complex redox systems are less studied. For instance, redox interactions in systems in which Fe(II) minerals dissolve while simultaneously precipitating iron(III) (hydr)oxides are not well understood.

Furthermore, additional Fe<sup>3+</sup> can be introduced into groundwater systems through anthropogenic means, such as the injection of treated wastewater during managed aquifer recharge (MAR) or in energy exploration water disposal.<sup>9,10</sup>

Received: July 23, 2015

Revised: December 5, 2015

Accepted: December 7, 2015

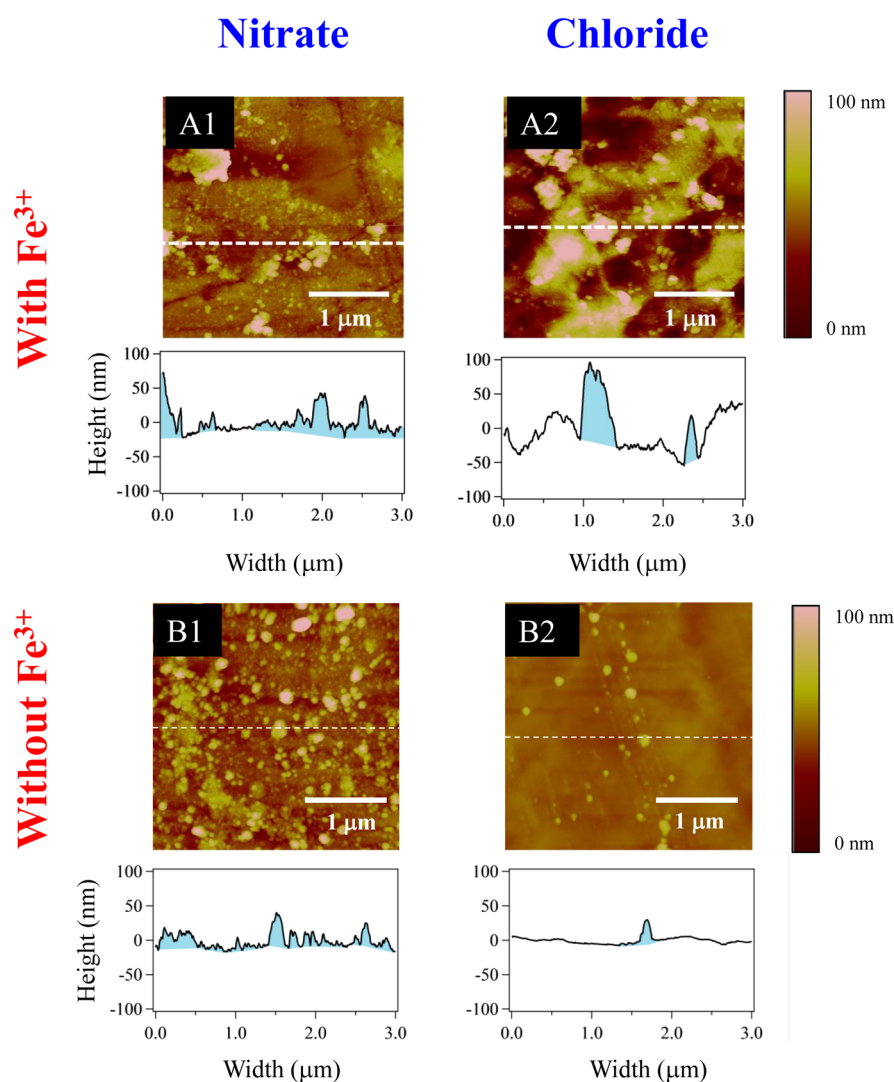


**Figure 1.** AFM height images for arsenopyrite flat coupons reacted for 7 days in batch reaction mixtures containing  $1.5 \mu\text{M Fe}^{3+}$  and 10 mM sodium nitrate (A1),  $1.5 \mu\text{M Fe}^{3+}$  and 10 mM sodium chloride (A2), 10 mM sodium nitrate (B1), and 10 mM sodium chloride (B2). The colored area under the AFM line cuts indicates where on the surface there appears to be secondary mineral precipitation compared to the background roughness.

The quality of water used during MAR varies greatly from resident groundwater because of the presence of oxidants such as dissolved oxygen and  $\text{Fe}^{3+}$ , and arsenic can become mobilized as a result.<sup>6,16–23</sup>

Thus, this study examines how the presence of low additional  $\text{Fe}^{3+}$  concentrations, comparable to those found in reclaimed water used for MAR, will influence arsenopyrite oxidation and secondary mineral phase formation.<sup>10</sup> While previous studies have tested the ability of dissolved  $\text{Fe}^{3+}$  species to oxidize arsenopyrite,<sup>7,24</sup> most were conducted under low-pH conditions, as dissolved  $\text{Fe}^{3+}$  species have decreased solubility at higher pHs. However, Moses et al. found that at higher pHs, the oxidation of pyrite, a related iron sulfide mineral, by aqueous  $\text{Fe}^{3+}$  was 1 order of magnitude higher than oxidation by dissolved oxygen.<sup>25</sup> They hypothesized that at higher pHs, aqueous  $\text{Fe}^{3+}$  exists as a hydroxo- $\text{Fe}^{3+}$  complex that can still act as an effective oxidant.

The circumneutral oxidation of arsenopyrite by aqueous  $\text{Fe}^{3+}$  species is crucial. This pH range is more environmentally relevant than those in previous studies, and these geochemical reactions can trigger the release of toxic arsenic into groundwater resources. While higher or lower pH conditions

can occur in specific scenarios such as acid mine drainage, circumneutral pH conditions are more common and can provide a basis for studying other extreme pH scenarios. Furthermore, the study by Moses et al. of pyrite oxidation by  $\text{Fe}^{3+}$  did not consider secondary mineral formation, which can act as a sink for aqueous arsenic in real systems.

Moreover, no studies have examined the simultaneous effects of  $\text{Fe}^{3+}$  on arsenic mobilization, secondary mineral precipitation, or phase transformation under the circumneutral pH conditions observed in most natural and engineered aquatic systems. Both the formation and phase transformation of iron(III) (hydr)oxide minerals can significantly impact the fate and transport of arsenic where the oxidative dissolution of arsenopyrite is a concern. The study presented here not only addresses these knowledge gaps but also delineates how complex Fe(II)–Fe(III) interactions, which can occur under dynamic redox conditions, influence arsenic mobilization from arsenic-containing iron(II) sulfide minerals.

## ■ MATERIALS AND METHODS

**Investigation of Arsenic Mobilization from Arsenopyrite.** Arsenic mobilization from arsenopyrite powder was

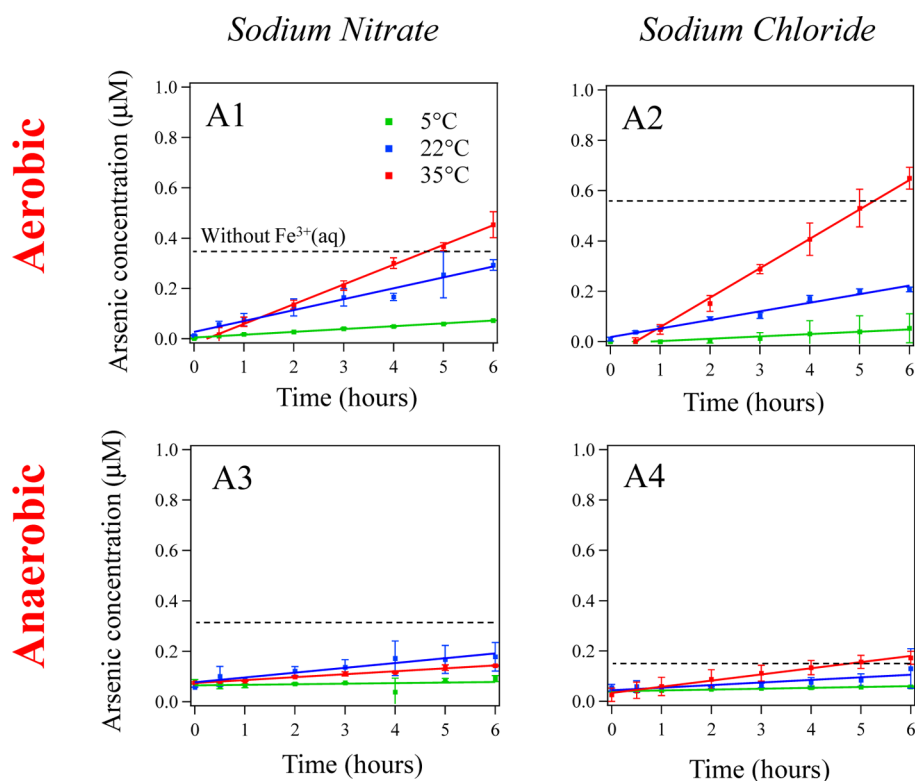


**Figure 2.** Arsenic concentration evolution for batch reactors containing arsenopyrite powder and  $1.5 \mu\text{M Fe}^{3+}$  over a 6 h reaction period for aerobic sodium nitrate (A1), aerobic sodium chloride (A2), anaerobic sodium nitrate (A3), and anaerobic sodium chloride (A4). The dotted lines indicate the maximal concentrations seen for the reactors without added  $\text{Fe}^{3+}$  at  $35^\circ\text{C}$  for each system. These dotted line values can be found in our previous work.<sup>10</sup>

monitored under aerobic and anaerobic conditions for systems containing either 10 mM sodium nitrate and  $1.5 \mu\text{M Fe}^{3+}$  or 10 mM sodium chloride and  $1.5 \mu\text{M Fe}^{3+}$ , concentrations comparable to levels measured in tertiary treated wastewater samples.<sup>10</sup> Aqueous samples were taken from triplicate batch reactors at 1 h intervals for 6 h. Arsenic concentrations were measured using inductively coupled plasma-mass spectroscopy (ICP-MS). The batch reactor temperature was varied from 5 to  $35^\circ\text{C}$  to calculate activation energies (Table S1 of the Supporting Information). The results from these experiments were compared with our previously published data on arsenic mobilization in systems without added  $\text{Fe}^{3+}$  containing either 10 mM sodium nitrate or 10 mM sodium chloride under aerobic and anaerobic conditions.<sup>10</sup> Thus, a total of eight systems were included in our experimental data set.

The nature of  $\text{Fe}^{3+}$  in our system was investigated using MINEQL+ (version 4.6). We found that when the formation of ferrihydrite is considered, only  $3.95 \times 10^{-9} \text{ M Fe}(\text{OH})_2^+$  is soluble for both the nitrate and chloride systems. Considering only the aqueous phase species, 90% of iron exists as  $\text{Fe}(\text{OH})_2^+$  and 10% existed as  $\text{Fe}(\text{OH})_3^0(\text{aq})$  for both systems. However, these calculations assume that the system is at equilibrium. Because the real system may have kinetic limitations, dissolved  $\text{Fe}^{3+}$  species can exist as aqueous complexes at concentrations higher than equilibrium values. For example, Dousma and Bruyn<sup>26</sup> studied the hydrolysis of a ferric nitrate solution and found that, while the formation of smaller polymeric species occurred quickly, larger polymers formed relatively slowly. In addition to dissolved species,  $\text{Fe}^{3+}$  can also be present as colloidal  $\text{Fe}(\text{III})$  phases. These  $\text{Fe}^{3+}$  species can potentially react with arsenopyrite and form iron(III) (hydr)oxide

secondary mineral precipitates, as described later in our proposed reaction mechanism.

#### Investigation of Secondary Mineral Formation.

Quantities and the morphology of secondary mineral phases were determined using a combination of atomic force microscopy (AFM), to assess the surface coverage, and citrate–bicarbonate–dithionite (CBD) extraction, to quantify the total amount of precipitated  $\text{Fe}(\text{III})$  phases.<sup>27</sup> Raman spectroscopy at a low magnification was used to identify secondary mineral phases.<sup>10</sup> While the low magnification prevented artificial aging of precipitates by the Raman laser, acquired spectra still show the secondary minerals clearly. Tests also confirmed that Raman did not cause phase transformation of iron(III) (hydr)oxides (Figure S2 of the Supporting Information). For these experiments, flat polished arsenopyrite “coupons” were placed in the described batch reactors at room temperature and allowed to react for up to 14 days. X-ray diffraction (XRD) and transmission electron microscopy (TEM) analyses of these systems were not feasible because our experiments were conducted on a flat substrate.

Our experimental methods are detailed in the Supporting Information.

## RESULTS AND DISCUSSION

We found that the effects of  $\text{Fe}^{3+}$  on arsenopyrite oxidative dissolution are threefold.

**More Secondary Mineral Precipitation in Additional  $\text{Fe}^{3+}$  Systems.** AFM images (Figure 1) show significantly more precipitation in the systems with additional  $\text{Fe}^{3+}$  after 7 days compared to the systems without  $\text{Fe}^{3+}$ .<sup>10</sup> With additional  $\text{Fe}^{3+}$ , precipitation was smaller (10–50 nm height;  $N > 100$

precipitates) in the sodium nitrate system than in the sodium chloride system (50–100 nm;  $N > 50$  precipitates). For the sodium chloride system with  $\text{Fe}^{3+}$ , the surface was much rougher (RMS = 3.51 nm without added  $\text{Fe}^{3+}$ , compared to 23.9 nm with added  $\text{Fe}^{3+}$ ), indicating more extensive dissolution and secondary mineral precipitation. Interestingly, in the absence of  $\text{Fe}^{3+}$ , there was less precipitation observed for the chloride system (Figure 1B2) than for the nitrate system (Figure 1B1). This mechanism is explored further later in the manuscript.

The AFM observations are consistent with CBD measurements of the total Fe(III) phases precipitated on arsenopyrite powder after 7 days. Even after subtraction of the  $\text{Fe}^{3+}$  initially added to batch reactors (0.375  $\mu\text{mol}$  of  $\text{Fe}^{3+}$  per batch reactor), the total precipitated Fe(III) phases quantities per reactor were  $2.45 \pm 0.30$  and  $2.81 \pm 0.14 \mu\text{mol}$  of  $\text{Fe}(\text{OH})_3$  for the nitrate and chloride systems, respectively. Without additional  $\text{Fe}^{3+}$ , the total quantities were  $0.69 \pm 0.0015$  and  $0.65 \pm 0.14 \mu\text{mol}$  of  $\text{Fe}(\text{OH})_3$  for the nitrate and chloride systems, respectively. Thus, the addition of  $\text{Fe}^{3+}$  led to more extensive precipitation.

**Higher Arsenic Mobilization in Additional  $\text{Fe}^{3+}$  Systems.** As shown in Figure 2, after 6 h with added 1.5  $\mu\text{M}$   $\text{Fe}^{3+}$ , the concentration of arsenic increased to a maximum of  $0.45 \pm 0.05 \mu\text{M}$  for the sodium nitrate system and  $0.65 \pm 0.06 \mu\text{M}$  for the sodium chloride system under aerobic conditions at the highest temperature, 35 °C. These values represent a 36% increase in arsenic concentration for the nitrate system and an 18% increase for the chloride system compared to same systems without added  $\text{Fe}^{3+}$ .<sup>10</sup> We also expect that for the aerobic systems at 35 °C, the impacts of secondary mineral formation on arsenic concentration are the most exaggerated, as previous testing has showed increased iron(III) (hydr)oxide precipitation at higher temperatures (Figure S3 of the Supporting Information). While the differences in arsenic concentration are not striking, particularly for lower temperatures, the increase is troubling in the context of the increased secondary mineral formation in  $\text{Fe}^{3+}$ -containing systems. Our results indicate that these minerals may not be a sufficiently effective sink to entirely mitigate arsenic, despite their large quantity.

To test whether the increases in arsenic concentration could be due to increased oxidation of arsenopyrite by  $\text{Fe}^{3+}$  in addition to dissolved oxygen, these experiments were repeated under anaerobic conditions. Interestingly, the maximal arsenic concentrations for the anaerobic nitrate and chloride systems containing  $\text{Fe}^{3+}$  were  $0.17 \pm 0.02$  and  $0.18 \pm 0.06 \mu\text{M}$  (Figure 2A3 and 2A4), respectively. These values were similar, for the chloride case, or even lower, for the nitrate case, than those of the anaerobic systems without additional  $\text{Fe}^{3+}$ , indicating that for circumneutral pH conditions in the absence of dissolved oxygen,  $\text{Fe}^{3+}$  is not able to oxidize arsenopyrite to a significant extent.<sup>10</sup>

The increased arsenic concentration under aerobic conditions thus cannot be attributed to the oxidation of arsenopyrite by  $\text{Fe}^{3+}$ , even though additional  $\text{Fe}^{3+}$  increased secondary mineral formation. Possibly without dissolved oxygen, the concentration of  $\text{Fe}^{3+}$  was not high enough to mobilize arsenic from arsenopyrite: The added  $\text{Fe}^{3+}$  concentration was only 1.5  $\mu\text{M}$ , compared to a dissolved oxygen concentration of 6.19 mM. However, it is clear that when  $\text{Fe}^{3+}$  and dissolved oxygen coexist during arsenopyrite oxidative dissolution, both iron(III) (hydr)oxide formation and arsenic release are increased. We explore this mechanism further below.

**Faster Secondary Mineral Phase Transformation with Additional  $\text{Fe}^{3+}$ .** Although the addition of  $\text{Fe}^{3+}$  increased secondary mineral precipitation, this increase did not entirely mitigate arsenic mobility, but rather arsenic concentrations were increased. Mobilized arsenic quantities may exceed what can be attenuated by secondary minerals. In addition, the sorption capacity of these minerals is related to their phase. Thus, to determine the process responsible, the phase of the secondary minerals was investigated using Raman spectroscopy (Figure 3). In our previous study without additional  $\text{Fe}^{3+}$ , only

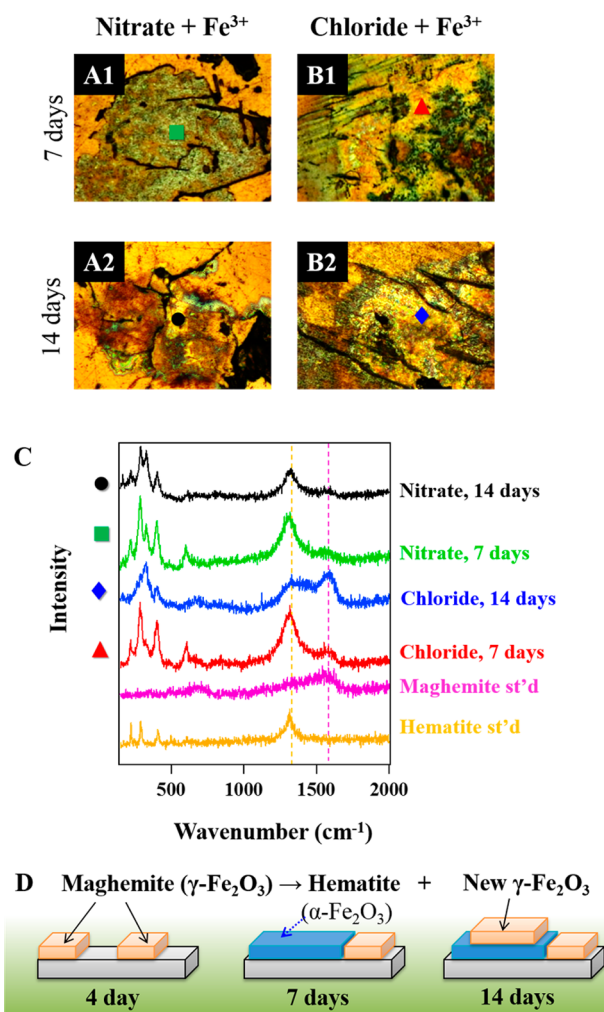


**Figure 3.** Optical microscope images of the arsenopyrite coupon reacted in systems containing 1.5  $\mu\text{M}$   $\text{Fe}^{3+}$  and 10 mM sodium nitrate for 7 days (A1) and 14 days (A2), or 1.5  $\mu\text{M}$   $\text{Fe}^{3+}$  and 10 mM sodium chloride for 7 days (B1) and 14 days (B2). Colored symbols indicate where the Raman spectra (C) were taken. Maghemite was the dominant phase identified for the 14 day sample from the chloride system, while for all other systems, hematite was the dominant phase. The macro-scale mechanism for secondary mineral phase transformation is shown in panel D. The spectra for ferrihydrite can be found in Figure S4 of the Supporting Information.

maghemite was observed on the arsenopyrite surface for the nitrate system, while both maghemite and hematite were observed for the chloride system. Furthermore, for the nitrate system, only maghemite was observed, even after reaction for 14 days.<sup>10</sup>

For both systems with additional  $\text{Fe}^{3+}$ , maghemite was the first detectable secondary phase after 4 days. By 7 days, the

maghemite had undergone phase transformation, becoming hematite. With an increase in time, maghemite precipitates were again observed on the surface of these coupons, even on areas coated in the blueish precipitates. These blueish precipitates were consistently identified as hematite during our previous study of arsenopyrite oxidation.<sup>10</sup> Additional CBD analysis conducted on arsenopyrite powder reacted for 14 days showed that the iron(III) (hydr)oxide precipitate quantities per batch reactor increased with time from  $2.83 \pm 0.30 \mu\text{mol}$  at 7 days to  $3.36 \pm 0.17 \mu\text{mol}$  at 14 days for the nitrate system and from  $3.19 \pm 0.14 \mu\text{mol}$  at 7 days to  $3.47 \pm 0.28 \mu\text{mol}$  at 14 days for the chloride system. If the phase transformation of hematite back into maghemite were the main mechanism, the total Fe(III) precipitate quantity would not increase. Thus, we concluded that the observed maghemite spectrum results from maghemite precipitates forming on surfaces already coated with hematite (Figure 3D). These Raman observations show that additional  $\text{Fe}^{3+}$  not only led to increased precipitation but also accelerated phase transformation.

**Mechanism of  $\text{Fe}^{3+}$ –Arsenopyrite Interactions.** We propose a mechanism analogue to the discussion by Moses and Herman for circumneutral pyrite oxidation.<sup>28</sup> First, the additional  $\text{Fe}^{3+}$  can sorb on the surface.  $\text{Fe}^{\text{II}}$  in the mineral can then donate its electron to  $\text{Fe}^{3+}$ , forming  $\text{Fe}^{\text{III}}$  and either directly reducing  $\text{Fe}^{3+}$  to  $\text{Fe}^{2+}$  or forming a  $\text{Fe}^{2+}/\text{Fe}^{3+}$  complex with a delocalized electron. This  $\text{Fe}^{2+}$  or  $\text{Fe}^{2+}/\text{Fe}^{3+}$  complex will donate its electron to dissolved oxygen, forming  $\text{Fe}^{3+}$  again and repeating the cycle. With time,  $\text{Fe}^{\text{III}}$  on the surface will form iron(III) (hydr)oxide secondary mineral precipitates. The phase transformation of these minerals can be accelerated because of electron transfer and atom exchange between  $\text{Fe}^{2+}$  and  $\text{Fe}^{3+}$ , and the precipitation extents will be greatly increased due to the increased oxidative dissolution by  $\text{Fe}^{3+}$ . Colloidal Fe(III) phases can also potentially adsorb onto the arsenopyrite surface and undergo phase transformation to form more aged iron(III) (hydr)oxide minerals such as maghemite.<sup>29</sup> This phase transformation can be accelerated by  $\text{Fe}^{2+}$  present from arsenopyrite dissolution. However, even if all of the added  $\text{Fe}^{3+}$  formed Fe(III) colloids that deposited on the arsenopyrite surface, this could account only for less than 12 and 13% of the total precipitated secondary Fe(III) minerals for the chloride and nitrate systems, respectively. Therefore, this mechanism may be less significant than precipitation which forms during the oxidation of arsenopyrite.

During this oxidation process, arsenic can be dissolved from the exposed arsenopyrite surface. Even after reaction for 14 days, there was still some arsenopyrite surface exposed to the solution that could be seen using the Raman optical microscope. However, dissolution may become slower as more of the surface is coated in secondary minerals.

In addition, if iron(III) (hydr)oxide solids on the arsenopyrite surface become charged with Fe(II) due to the delocalization of electrons, they can be continuously oxidized by dissolved oxygen, which explains the increased precipitation quantities even after 14 days, when the surface is coated by precipitates. Electron transfer kinetics can also be different in the presence of these iron(III) (hydr)oxides. For example, if electron transfer from arsenopyrite to maghemite to oxygen is faster than transfer from arsenopyrite to oxygen, oxidation can occur more rapidly. Furthermore, because the electrical conductivity of sodium chloride exceeds that of sodium nitrate at ambient temperatures, electron transfer would be faster in sodium chloride than in sodium nitrate.<sup>30</sup> Thus, this

mechanism bolsters our observation of faster dissolution and more extensive precipitation in the chloride system compared to the nitrate system (Figure 1A1 and 1A2).

Our findings call immediate attention to the role of additional  $\text{Fe}^{3+}$  in arsenopyrite oxidative dissolution kinetics at circumneutral pHs. We have found that aqueous  $\text{Fe}^{3+}$  species can still be highly reactive toward arsenopyrite, resulting in both faster dissolution and more extensive secondary mineral precipitation. These species can be present along with precipitating iron(III) (hydr)oxides as the system approaches equilibrium. Future investigations are needed to delineate the exact mechanism of reaction, including (1) the potential formation of  $\text{Fe}^{2+}/\text{Fe}^{3+}$  complexes and (2) the fate of sulfur and arsenic speciation from arsenopyrite in our experimental systems. This study provides insight into arsenic transport in aquatic systems, where the quantities and phase of iron(III) (hydr)oxides can significantly impact arsenic concentrations. These findings also have vital implications for MAR, where  $\text{Fe}^{3+}$  can be introduced along with dissolved oxygen to subsurface systems containing arsenic-bearing sulfides.

## ■ ASSOCIATED CONTENT

### 📄 Supporting Information

The Supporting Information is available free of charge on the ACS Publications website at DOI: 10.1021/acs.estlett.5b00311.

Experimental descriptions, four figures, and one table (PDF)

## ■ AUTHOR INFORMATION

### Corresponding Author

\*E-mail: [ysjun@seas.wustl.edu](mailto:ysjun@seas.wustl.edu). Phone: (314)935-4539. Fax: (314)935-7211.

### Notes

The authors declare no competing financial interest.

## ■ ACKNOWLEDGMENTS

We are grateful for support received from the National Science Foundation (EAR-1424927). C.W.N. acknowledges the support of the Mr. and Mrs. Spencer T. Olin Fellowship. We thank Environmental NanoChemistry Group members for valuable discussion. We also thank Prof. Jim Ballard for carefully reviewing our manuscript.

## ■ REFERENCES

- (1) Smedley, P. L.; Kinniburgh, D. G. A review of the source, behaviour and distribution of arsenic in natural waters. *Appl. Geochem.* **2002**, *17* (5), 517–568.
- (2) Utsunomiya, S.; Peters, S. C.; Blum, J. D.; Ewing, R. C. Nanoscale mineralogy of arsenic in a region of New Hampshire with elevated As-concentrations in the groundwater. *Am. Mineral.* **2003**, *88* (11–12), 1844–1852.
- (3) Nickson, R.; McArthur, J.; Ravenscroft, P.; Burgess, W.; Ahmed, K. Mechanism of arsenic release to groundwater, Bangladesh and West Bengal. *Appl. Geochem.* **2000**, *15* (4), 403–413.
- (4) Postma, D.; Larsen, F.; Minh Hue, N. T.; Duc, M. T.; Viet, P. H.; Nhan, P. Q.; Jessen, S. r. Arsenic in groundwater of the Red River floodplain, Vietnam: controlling geochemical processes and reactive transport modeling. *Geochim. Cosmochim. Acta* **2007**, *71* (21), 5054–5071.
- (5) Meng, X.; Jing, C.; Korfiatis, G. P. In *A review of redox transformation of arsenic in aquatic environments*; ACS Symposium Series; American Chemical Society: Washington, DC, 2003; pp 70–83.

- (6) Jones, G. W.; Pichler, T. Relationship between pyrite stability and arsenic mobility during aquifer storage and recovery in southwest central Florida. *Environ. Sci. Technol.* **2007**, *41* (3), 723–730.
- (7) Yu, Y.; Zhu, Y.; Gao, Z.; Gammons, C. H.; Li, D. Rates of Arsenopyrite Oxidation by Oxygen and Fe(III) at pH 1.8 - 12.6 and 15 - 45 °C. *Environ. Sci. Technol.* **2007**, *41* (18), 6460–6464.
- (8) Neil, C. W.; Lee, B.; Jun, Y.-S. Different Arsenate and Phosphate Incorporation Effects on the Nucleation and Growth of Iron(III) (Hydr)oxides on Quartz. *Environ. Sci. Technol.* **2014**, *48* (20), 11883–11891.
- (9) Neil, C. W.; Yang, Y. J.; Jun, Y.-S. Arsenic mobilization and attenuation by mineral-water interactions: implications for managed aquifer recharge. *J. Environ. Monit.* **2012**, *14* (7), 1772–1788.
- (10) Neil, C. W.; Yang, Y. J.; Schupp, D.; Jun, Y.-S. Water Chemistry Impacts on Arsenic Mobilization from Arsenopyrite Dissolution and Secondary Mineral Precipitation: Implications for Managed Aquifer Recharge. *Environ. Sci. Technol.* **2014**, *48* (8), 4395–4405.
- (11) Rosso, K. M.; Yanina, S. V.; Gorski, C. A.; Larese-Casanova, P.; Scherer, M. M. Connecting observations of hematite ( $\text{Fe}_2\text{O}_3$ ) growth catalyzed by Fe (II). *Environ. Sci. Technol.* **2010**, *44* (1), 61–67.
- (12) Boland, D.; Collins, R. N.; Miller, C. J.; Glover, C. J.; Waite, T. D. Effect of solution and solid-phase conditions on the Fe (II)-accelerated transformation of ferrihydrite to lepidocrocite and goethite. *Environ. Sci. Technol.* **2014**, *48*, 5477.
- (13) Pedersen, H. D.; Postma, D.; Jakobsen, R.; Larsen, O. Fast transformation of iron oxyhydroxides by the catalytic action of aqueous Fe (II). *Geochim. Cosmochim. Acta* **2005**, *69* (16), 3967–3977.
- (14) Yang, L.; Steefel, C. I.; Marcus, M. A.; Bargar, J. R. Kinetics of Fe (II)-catalyzed transformation of 6-line ferrihydrite under anaerobic flow conditions. *Environ. Sci. Technol.* **2010**, *44* (14), 5469–5475.
- (15) Frierdich, A. J.; Catalano, J. G. Controls on Fe (II)-activated trace element release from goethite and hematite. *Environ. Sci. Technol.* **2012**, *46* (3), 1519–1526.
- (16) Dillon, P. Future management of aquifer recharge. *Hydrogeol. J.* **2005**, *13* (1), 313–316.
- (17) Hollander, H.; Mull, R.; Panda, S. A concept for managed aquifer recharge using ASR-wells for sustainable use of groundwater resources in an alluvial coastal aquifer in Eastern India. *Phys. Chem. Earth, Pt A/B/C* **2009**, *34* (4), 270–278.
- (18) Foster, S. S.; Garduno, H.; Tuinhof, A.; Kemper, K.; Nanni, M. Urban wastewater as groundwater recharge: Evaluating and managing the risks and benefits. In *GW-MATE Briefing Note Series*; Banco Mundial: 2003; Vol. 12.
- (19) Arthur, J.; Dabous, A.; Cowart, J. Water-rock geochemical considerations for aquifer storage and recovery: Florida case studies. *Dev. Water Sci.* **2005**, *52*, 327–339.
- (20) Lazareva, O.; Druschel, G.; Pichler, T. Understanding arsenic behavior in carbonate aquifers: Implications for aquifer storage and recovery (ASR). *Appl. Geochem.* **2015**, *52*, 57–66.
- (21) Mirecki, J. E.; Bennett, M. W.; Lopez-Balaz, M. C. Arsenic Control During Aquifer Storage Recovery Cycle Tests in the Floridan Aquifer. *Groundwater* **2013**, *51* (4), 539–549.
- (22) Mirecki, J. E. Geochemical Models of Water-Quality Changes During Aquifer Storage Recovery (ASR) Cycle Tests, Phase 1: Geochemical Models Using Existing Data. DTIC Document, 2006.
- (23) Vanderzalm, J.; Dillon, P.; Barry, K.; Miotlinski, K.; Kirby, J.; Le Gal La Salle, C. Arsenic mobility and impact on recovered water quality during aquifer storage and recovery using reclaimed water in a carbonate aquifer. *Appl. Geochem.* **2011**, *26* (12), 1946–1955.
- (24) Corkhill, C. L.; Vaughan, D. J. Arsenopyrite oxidation - A review. *Appl. Geochem.* **2009**, *24* (12), 2342–2361.
- (25) Moses, C. O.; Kirk Nordstrom, D.; Herman, J. S.; Mills, A. L. Aqueous pyrite oxidation by dissolved oxygen and by ferric iron. *Geochim. Cosmochim. Acta* **1987**, *51* (6), 1561–1571.
- (26) Dousma, J.; De Bruyn, P. L. Hydrolysis-precipitation studies of iron solutions. I. Model for hydrolysis and precipitation from Fe(III) nitrate solutions. *J. Colloid Interface Sci.* **1976**, *56* (3), 527–539.
- (27) Mehra, O.; Jackson, M. In *Iron oxide removal from soils and clays by a dithionite-citrate system buffered with sodium bicarbonate*; National Conference on Clays and Clays Minerals, 1958; pp 317–327.
- (28) Moses, C. O.; Herman, J. S. Pyrite oxidation at circumneutral pH. *Geochim. Cosmochim. Acta* **1991**, *55* (2), 471–482.
- (29) Cornell, R. M.; Schwertmann, U. *The iron oxides: Structure, properties, reactions, occurrences and uses*; John Wiley & Sons: New York, 2006.
- (30) Haynes, W. M. *CRC handbook of chemistry and physics*; CRC Press: Boca Raton, FL, 2012.